



Research papers

Deterministic observability calculations for zero-dimensional models of lithium–sulfur batteries

Veronica Marchante Rodriguez, Neda Shateri*, Abbas Fotouhi, Karsten Propp, Daniel J. Auger

Advanced Vehicle Engineering Centre, Cranfield University, Bedfordshire MK43 0AL, UK



ARTICLE INFO

Keywords:

Lithium-sulfur battery
Analytical modelling
Numerical modelling
Observability matrix, state estimation

ABSTRACT

Among the various energy storage technologies under development, the lithium-sulfur (Li-S) battery has considerable promise due to its higher theoretical energy density, small environmental footprint, and low projected costs. One of the main challenges posed by Li-S is the need for a battery management system (BMS) that can accommodate the system's complex multi-step redox behaviours; conventional approaches for lithium-ion batteries do not transfer. Most existing approaches rely on equivalent circuit network models, but there is growing interest in 'zero-dimensional' electrochemical models which can potentially give insights into the relative polysulfide species concentrations present at any given time. To be useful for state estimation, a model must be 'observable': it must be possible to uniquely determine the internal state through observation of the system's behaviour over time. Previous studies have assessed observability using numerical methods, which is an approximation. This study derives an analytic expression for the observability criterion, which allows greater confidence in the results. The analytic observability criterion is then validated against a numerical comparator. A zero-dimensional model from the literature is translated into an ordinary differential equation (ODE) form to define the state variables matrix A , the output matrix C , and subsequently the observability matrix O . These are compared to simulated numerical equivalents. In addition, the sensitivity of the numerical process has been demonstrated. The results have the potential to offer greater confidence in conclusions around observability, which in turn gives greater confidence in the effects of any algorithms based on them.

1. Introduction

Lithium-sulfur (Li-S) is considered to be a promising technology for the next generation of batteries due to properties such as high theoretical specific energy of 2600 Wh/kg (practically around 300 Wh/kg today, projected to rise in the future), low toxicity, low cost, and the abundance of sulfur [1,2]. The high specific energy of Li-S batteries is a consequence of multi-step electrochemical conversion reactions of polysulfides in different valence states where sulfur is reduced on the cathode to produce lithium polysulfides (Li_2S_i) intermediates (e.g. Li_2S_6 , Li_2S_4 , Li_2S_2). Despite lithium-sulfur batteries' promise, several problems make the commercialization of Li-S batteries difficult, as is acknowledged in the literature [1,3,4]. The use of Li-S battery is currently limited by its low charge efficiency and relatively high self-discharge rate, however, its inherent safety is an advantage in some niche applications [3]–[5]. In the following, some of the technical challenges of the Li-S battery are listed:

- The dissolution of intermediate Li_2S_i in the liquid electrolyte can lead to migration through the separator. This subsequently creates a shuttle effect and leads to Li_2S deposition on the Li anode, resulting in a loss of active substances and poor cycle life.
- The low electrical conductivity of sulfur (ca. 10^{-30} Sm^{-1}) as well as the associated discharge products (e.g. Li_2S , ca. 10^{-14} Sm^{-1}) greatly hinder the transportation of e^-/Li^+ and decelerate the reaction kinetics in batteries.
- The conversion reaction between sulfur (2.07 gcm^{-3}) and Li_2S (1.66 gcm^{-3}) upon the delithiation/lithiation process involves a volume change of around 76 %, leading to severe disintegration of the electrodes and deterioration of the prolonged cycling performance.
- Li-S batteries inevitably face the intrinsic issues of mossy metal deposits and dendrite generated on the surface of the Li anode, as well as the unstable solid electrolyte interface (SEI), resulting in low coulombic efficiency (CE), terrible cycling, and severe safety concerns.

* Corresponding author.

E-mail address: neda.shateri@cranfield.ac.uk (N. Shateri).

<https://doi.org/10.1016/j.est.2024.111442>

Received 8 August 2023; Received in revised form 15 February 2024; Accepted 20 March 2024

Available online 29 March 2024

2352-152X/© 2024 The Authors. Published by Elsevier Ltd. This is an open access article under the CC BY license (<http://creativecommons.org/licenses/by/4.0/>).

There has been wide research focused on the selection of materials and architecture of electrodes and electrolytes to overcome the above-mentioned issues. The key aspect has been the interface between electrodes and the electrolyte. Different solutions have been suggested, and the use of solid-state electrolytes (SSEs) seems to be a promising route, as these can avoid leakage, reduce flammability and chemical instability and also provide a physical barrier to the polysulfide shuttle toward the Li anode [1].

Another challenge for the implementation and commercialization of Li–S batteries is the prediction of their performance during usage. In that regard, several researchers have investigated models to simulate the behaviour of Li–S batteries. Good examples are the Zero-Dimensional (0D) model, the One-Dimensional (1D) model, and other higher-dimensional models which are mentioned in the following. The first zero-dimensional model was proposed by Mikhaylik and Akridge [6] and it considered a 2-step reaction and the heat generation from the polysulfide shuttle effect. Some comprehensive models including diffusion limitations, activation of overpotentials, and precipitation of species have also been suggested in [7]. The zero-dimensional model developed by Marinescu et al. [3] is also based on the 2-step electrochemical reaction but with low computational requirements. That model is capable of simulating the typical features of this type of battery such as the two plateaus during discharge, the initial sharp increase in voltage during charge, the dynamic response of cells, the effect of current and power limitations, and information on the amount of stored energy. However, diffusion limitations are not considered in their model. In another study by Zhang et al. [8], a lumped model is developed for Li–S battery which includes precipitation and kinetics of the reactions and it considers the concentration dependency of electrolyte resistance. In that study, they extended the reaction mechanism to include all the generated polysulfide (S_n^{2-} , $n = 0, 2, 4, 6, 8$).

In addition to the zero-dimensional model, a number of Li–S battery modelling studies were focused on the 1D model which was originally proposed by Kumaresan et al. In that model, the Li–S cell was assumed to consist of two half cells where the electrochemical reactions take place at the two electrodes simultaneously. This modelling approach has been also supported in a study by Ghaznavi and Chen [9]. Following that, Zhang et al. developed a 1D model for Li–S battery based on Kumaresan's framework to study the transport limitations during discharge and also to analyze the capacity recovery at different rates [10]. In [11], Yoo et al. studied both discharge and charge processes by extending the precipitation/dissolution expressions in Kumaresan's model. They showed that the model can predict capacity loss, but it cannot be replicated, and the physics is not fully modelled using kinetics at the anode. In another study by Ren et al. [12], only the discharge process is considered in the 1D model by incorporating the surface nucleation and growth dynamics to study the precipitation of Li_2S . The charging process was also studied by Hofmann et al. [13], which assumed a simplified reaction mechanism by two-step redox reactions and a chemical precipitation reaction on the cathode side in their 1D model. Finally, Xiong et al. proposed a 1D transient mathematical model, which incorporates the size-dependent Li_2S dissolution and redox mediation reaction between dissolved polysulfides and Li_2S particles into the charging process [14].

One of the unique features of Li–S battery is its poor state observability [15]. Recent studies have looked into the application of the zero-dimensional electrochemical model proposed by Marinescu et al., [3] to address the observability of Li–S batteries. Huang et al., [16] applied the zero-dimensional electrochemical model and nonlinear differential equations for state estimation and suggested an extended Kalman filter. They confirmed that the states are locally observable and that the observability is weak in the so-called “low plateau” region. On the other hand, Xu et al. [17] proposed a reformulation into ordinary differential equations (ODEs) to simplify the state estimation, as well as the development of an unscented Kalman filter. They also concluded that

the “low plateau” region has poor observability. However, both these studies were constructed on numerical calculations for the observability of the system. To the best knowledge of the authors, an analytical formulation of the Li–S battery system's observability has not been addressed in the literature yet, which is considered here as a research gap. The difference between [16] and this study is that the observability has been evaluated here both numerically and analytically. Our research formally confirms this. The model in this paper is accurately expressed as an ODE without loss of information. DAEs have applications in modelling constraints, but here – where the only constraints are equivalence – there is an exact one-to-one mapping, and such is used in [16]. In fact, [16] converts from DAE to ODE, though the observability criterion is evaluated numerically. Our conclusion supports the methods in [16] by filling a gap in the formal proof. For a battery management problem, it is the local observability that is important. It might well be that a formal extension using Lie algebra and local sets could be of interest, but we are responding to techniques already under discussion in the literature. We are providing a formal proof of the observability criterion in [16].

The poor observability of the Li–S battery system has been also reported in some other previous studies using an equivalent circuit model. In [15,18], an observability analysis is performed in order to predict the state of charge (SOC) of Li–S batteries, and it is demonstrated that the system is not locally observable due to the characteristics of the open-circuit voltage (OCV) curve. They also worked on the development of an equivalent circuit model for a Li–S cell, validating against experimental results and concluding that the poor observability made this approach impractical. That highlighted the need for the generation of a new framework to address the observability of Li–S batteries.

The aim of this work is to provide an analytical solution to the evaluation of the Li–S battery system's observability. It is well-recognised that numerical approximations of mathematical problems are sensitive to the size of numerical perturbations, whereas analytic expressions are not [19]. An analytic model can therefore identify sensitivity problems or confirm they are not present. A zero-dimensional electrochemical model [3] has been used as a baseline for the development of the analytical formula for the state matrix A , and the output matrix C . Each step of the process has been validated against numerical solutions. Firstly, the numerical model for Li–S batteries has been compared to published data. Once verified, this numerical model has been used to determine the observability of the system, i.e. the observability matrix O , and to validate the analytical solution. The contributions of this study can be summarized as follows:

- A fundamental investigation of the Li–S battery system's observability is performed using the physics-based zero-dimensional model.
- An analytical state-space model is developed for observability analysis of the Li–S battery system.
- The results of the proposed model are compared against the numerical model's data. The authors' observation here is that it is always desirable to justify a numerical technique based on an algorithm – sometimes this can give useful insights into edge cases and it is perhaps less vulnerable to irregular numeric issues, but if there is good confirmation, it supports the decision to use a numerical technique.
- A sensitivity analysis is performed on the numerical results.

The main impact of this study is expected to be on the next-generation Li–S battery management systems (BMS). Present-day state estimation methods are heavily reliant on equivalent circuit models. This study helps us to achieve greater knowledge of the species concentrations and consequently provides greater insight and confidence about local observability in Li–S battery systems. The proposed state-space version of the physics-based zero-dimensional model has the potential to be implemented in BMS boards and consequently be utilized in real-time applications. Although the battery electrochemical models

are usually better in terms of accuracy, they might not be easily used in real-time applications because of their computational and memory requirements. The authors believe this study can contribute to achieving quicker commercialization of Li–S BMS technologies, which contributes in its way to overall efforts for electrification and decarbonization to support climate action and enable clean growth.

The structure of this paper is as follows, The modelling approach is described in Section 2, including: (a) the zero-dimensional electrochemical model for Li–S batteries, (b) the analytical model for the observability of the Li–S battery system, i.e. mathematical equations for A, C and O; and (c) description of the numerical model for the validation of the results. In Section 3, the results, validation and analytical and numerical calculations are explained; and finally, the conclusion and future work are discussed in Section 4.

2. Li–S battery model

The zero-dimensional electrochemical model developed by Marinescu et al. [3] and previously suggested by Mikhaylik and Akridge [6], is based on a two-step electrochemical reaction chain:



The first reaction represents the reduction of sulfur (S_8^0) and is related to the high voltage plateau shown in Fig. 1. This reaction will be denoted as reaction H in the following equations. Meanwhile, the second reaction, the reduction of S_4^{2-} , is linked to the low voltage plateau and denoted as reaction L in the following. The equilibrium potentials for each of the reaction (E_H and E_L) are given by the Nernst equations below:

$$E_H = E_H^0 + \frac{RT}{4F} \ln \left(f_H \frac{S_8^0}{(S_4^{2-})^2} \right) \quad (3)$$

$$E_L = E_L^0 + \frac{RT}{4F} \ln \left(f_L \frac{S_4^{2-}}{(S_2^{2-})^2} \right) \quad (4)$$

where E_H^0 and E_L^0 are the standard potentials for each reaction; F is the Faraday's constant; R is the ideal gas constant; T is the temperature; S_i represents the mass of each polysulfide; and f_H and f_L are constants to convert the concentration of the sulfur species to mass, calculated as follows:

$$f_H = \frac{n_{S_4}^2 M_{S_8} \nu}{n_{S_8}} \quad (5)$$

$$f_L = \frac{n_{S_2}^2 n_{S_4} M_{S_8}^2 \nu^2}{n_{S_4}} \quad (6)$$

where ν is the volume of electrolyte, M_{S_8} is the molar mass of sulfur and n_i are the atoms in each of the polysulfides (i.e. sulfur species).

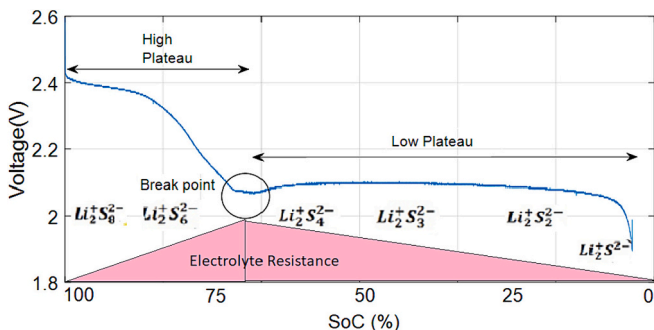


Fig. 1. Discharge voltage measurement of Li–S.

This model considers the kinetic limitations via the Butler-Volmer relation, so that the current linked to each reaction (i.e. i_H and i_L for the high and low plateaus) are given by:

$$i_H = -2 \bullet i_{H,0} \bullet a_r \sinh \frac{n_e F \eta_H}{2RT} \quad (7)$$

$$i_L = -2 \bullet i_{L,0} \bullet a_r \sinh \frac{n_e F \eta_L}{2RT} \quad (8)$$

where $i_{H,0}$ and $i_{L,0}$ are the exchange current densities for the high and low plateau reactions, respectively, a_r is the active surface of the cell, n_e is the number of electrons transferred in the reaction (in this case n_e is 4 for both reactions), and, i_H and i_L are current related to each reaction. The total current of the cell I is the summation of the currents for each reaction:

$$I = i_H + i_L \quad (9)$$

The surface overpotential is the driving force for the reactions, and it is defined as the difference between the voltage of the cell V and the equilibrium potential (E_H , E_L):

$$\eta_H = V - E_H \quad (10)$$

$$\eta_L = V - E_L \quad (11)$$

This zero-dimensional model considers the loss of efficiency due to the precipitation of sulfur as well as the shuttle phenomenon, which happens at high order polysulfides. That is related to the migration/diffusion of dissolved high-order polysulfides to the anode to form shorter polysulfides and return to the cathode. This process is repeated, resulting in deposition of non-conductive layers on the anode surface, thus reducing efficiency and capacity [20,21]. These processes are represented in the kinetic equations via kinetic constants k_s for the shuttle effect; and k_p for the precipitation. However, this model does not account for double layer effect/formation at the electrode/electrolyte interface.

The kinetic equations for variation of the amount of sulfur species with time, including the shuttle (k_s) and precipitation (k_p) effects [3], are:

$$\frac{dS_8^0}{dt} = -\frac{n_{S_8} M_{S_8}}{n_e F} i_H - k_s S_8^0 \quad (12)$$

$$\frac{dS_4^{2-}}{dt} = \frac{n_{S_8} M_{S_8}}{n_e F} i_H + k_s S_8^0 - \frac{n_{S_4} M_{S_8}}{n_e F} i_L \quad (13)$$

$$\frac{dS_2^{2-}}{dt} = \frac{n_{S_4} M_{S_8}}{n_e F} i_L \quad (14)$$

$$\frac{dS^{2-}}{dt} = \frac{2n_S M_{S_8}}{n_e F} i_L - \frac{1}{\nu \rho_S} k_p S_p (S^{2-} - S_s^{2-}) \quad (15)$$

$$\frac{dS_p}{dt} = \frac{1}{\nu \rho_S} k_p S_p (S^{2-} - S_s^{2-}) \quad (16)$$

where S_p is the mass of precipitated sulfur, ρ_S is the density of sulfur and S_s^{2-} is the saturation mass of sulfur (assumed to be constant, as long as the volume of the electrolyte, ν , remains constant).

All the previous Eqs. (3)–(16) are used to describe the electrochemical behaviour of the Li–S battery during charge and discharge processes. A list of the model's parameters is provided in Table 1, which is available in the literature [3]. It is not within the scope of this work to obtain these parameters, but this study responds to the existing models and shows how they might be used [22]. The 'big picture' for zero-dimensional lithium-sulfur model developments is nicely captured in [23]. We have used the model structure and parameters from a stable point in the literature [3]. As our contribution is based on algebra, the work that we do here will be generalizable as the model progresses, and

Table 1
Constant parameters for the Li–S battery model [3].

Parameter		Value	Units
F	Faraday's constant	9.649×10^4	C/mol
M_{S8}	Molar mass of sulfur	32	g/mol
N_A	Avogadro number	6.0221×10^{23}	1/mol
n_e	Electron number per reaction	4	–
$n_{S8}, n_{S4}, n_{S2}, n_S$	Number of S atoms in polysulfide	8, 4, 2, 1	–
R	Ideal gas constant	8.3145	J/K mol
ρ_s	Density of sulfur	2×10^3	g/L
a_r	Active reaction area per cell	0.960	m ²
f_H	Dimensionally factor for reaction H	0.7296	g/L/mol
f_L	Dimensionally factor for reaction L	0.0665	g ² L ² /mol
v	Volume of electrolyte per cell	0.0114	L
m_S	Total mass of active sulfur per cell	2.7	g
E_H^0	Standard potential of reaction H	2.35	V
E_L^0	Standard potential of reaction L	2.195	V
$i_{H,0}$	Exchange current density reaction H	1	A/m ²
$i_{L,0}$	Exchange current density reaction L	0.5	A/m ²
S_8^{2-}	Saturation mass for S ²⁻	0.0001	g
k_p	Precipitation rate	100	1/s
k_s	Shuttle constant	0.0002	1/s
T	Temperature	298	K

the methods and findings of this work will hold equally true for other parameter values. It should be noted that the parameters presented in Table 1 [3], are obtained for a fresh 3.4 Ah Li–S cell. Therefore they might not be valid for another type of Li–S cell or either for the same cell once it gets aged. Therefore, before any real-time application of this model, off-line parameterisation of the model is necessary.

3. Analytical/mathematical model for the observability of Li–S batteries

The general formulation of a continuous linear dynamic system is:

$$\dot{x}(t) = A(t)x(t) + B(t)u(t) \quad (17)$$

$$y(t) = C(t)x(t) + D(t)u(t) \quad (18)$$

where $t \in \mathbb{R}$ denotes the time, $x(t) \in \mathbb{R}^n$ is the state, $u(t) \in \mathbb{R}^m$ is the input or control, $y(t) \in \mathbb{R}^p$ is the output, $A(t) \in \mathbb{R}^{n \times n}$ is the dynamics or state matrix, $B(t) \in \mathbb{R}^{n \times m}$ is the input matrix, $C(t) \in \mathbb{R}^{p \times n}$ is the output or sensor matrix, and $D(t) \in \mathbb{R}^{p \times m}$ is the feedthrough matrix. The system would be observable if (and only if) the value of the initial state $x(t_0)$ can be determined from the system output $y(t)$ that has been observed through the time interval $(t_0 < t < t_f)$. If the system is observable, then the internal state variables $x(t)$ can be externally measured.

The observability of the system only depends on the state matrix A and the output matrix C . The observability matrix O is defined as follows:

$$O = \begin{bmatrix} C \\ CA \\ CA^2 \\ \vdots \\ CA^{n-1} \end{bmatrix} \quad (19)$$

The system would be observable if the rank of this matrix is the same as the order of the state variable $x(t)$, in this case “ n ” (as $x(t) \in \mathbb{R}^n$).

In the case of Li–S battery, the system can be formulated as follows:

$$\dot{S}_i(t) = \frac{\partial S_i}{\partial t} = AS_i(t); S_i \in \mathbb{R}^4 \quad (20)$$

$$V(t) = CS_i(t); V \in \mathbb{R} \quad (21)$$

where $S_i(t)$ represents variation of the sulfur species' mass with time ($S_i = [S_8, S_4^{2-}, S_2^{2-}, S^{2-}]$), which is the state vector; and the cell's voltage, $V(t)$, which is the output. It should be noted that the precipitated sulfur (S_p) is omitted from the state vector since it can be calculated from the mass balance equation. In this case, the observability matrix O is given by:

$$[O] = \begin{bmatrix} C \\ CA \\ CA^2 \\ CA^3 \end{bmatrix} \quad (22)$$

In order to determine the observability matrix, analytical formulations for the state and output matrices have been obtained based on the zero-dimensional electrochemical model presented by Marinescu et al. [3]. In Li–S batteries, ‘state of charge’ is not a scalar quantity – the states are a list of species concentrations. The current zero-dimensional models in the literature do not represent spatial dynamics. On the other hand, an equivalent circuit network (ECN) model is an approximation of the time lags associated with spatial dynamics and is usually parameterized as a function of the SOC. There is not a straightforward relationship between the two models at this time. Consequently, the existing observability analyses using ECN models in the literature [15] are not useable here.

3.1. Analytical definition of the state matrix A

The terms of the state matrix A can be calculated as the partial derivatives of the variation of the input variables with respect to the time as follows:

$$a_{ij} = \frac{\partial}{\partial S_j} \left(\frac{dS_i}{dt} \right) \quad (23)$$

The kinetic equations Eqs. (12)–(16) represent variation of the mass of sulfur species with respect to the time. In this formulation, the elements 1, 2, 3 and 4 are assigned to the sulfur species S_8^0 , S_4^{2-} , S_2^{2-} and S^{2-} , respectively (Eqs. (12)–(15)). As an example, the first element of the matrix A is obtained as follows:

$$a_{11} = \frac{\partial}{\partial S_8^0} \left(\frac{dS_8^0}{dt} \right) = \frac{\partial}{\partial S_8^0} \left(-\frac{n_{S8} M_{S8} i_H}{n_e F} - k_s S_8^0 \right) = -k_s \quad (24)$$

Therefore, the terms of the state matrix A can be mathematically obtained using the partial derivatives of these equations as follows:

$$A = \begin{pmatrix} -k_s & 0 & 0 & 0 \\ k_s & 0 & 0 & 0 \\ 0 & 0 & 0 & 0 \\ 0 & 0 & 0 & \frac{-k_p S_p}{v \rho_s} \end{pmatrix} \quad (25)$$

3.2. Analytical definition of the output matrix C

To define the elements of the output matrix C , the following definition is used:

$$C = \begin{bmatrix} \frac{\partial g_1}{\partial x} \\ \vdots \\ \frac{\partial g_p}{\partial x} \end{bmatrix} \text{ or } C = \left[\frac{\partial g_1}{\partial x} \quad \dots \quad \frac{\partial g_p}{\partial x} \right] \quad (26)$$

where “ g ” is a function that relates the output (y) with the state variables

(x) and the input (u), i.e. $y = g(x, u)$. Following this definition, the output matrix **C** is obtained by deriving the output variable (V) with respect to each of the state variables (S_i):

$$C = \begin{bmatrix} \frac{dV}{dS_8} \\ \frac{dV}{dS_4^{2-}} \\ \frac{dV}{dS_2^{2-}} \\ \frac{dV}{dS^{2-}} \end{bmatrix} \text{ or } C = \begin{bmatrix} \frac{dV}{dS_8} & \frac{dV}{dS_4^{2-}} & \frac{dV}{dS_2^{2-}} & \frac{dV}{dS^{2-}} \end{bmatrix} \quad (27)$$

Using the relation of voltage (V) with the equilibrium potential for the oxidation of sulfur (S_8) (i.e. E_H) and the overpotential (η_H), it is possible to determine the partial derivatives of the voltage during the discharge process as follows:

$$V = E_H + \eta_H \quad (28)$$

$$\frac{dV}{dS_i} = \frac{d}{dS_i}(E_H + \eta_H) = \frac{dE_H}{dS_i} + \frac{d\eta_H}{dS_i} \quad (29)$$

Partial derivatives for the equilibrium potential ($\frac{dE_H}{dS_i}$) can be obtained from the Nernst equation that relates the equilibrium potential of the reaction with the chemical species (Eqs. (3) and (4)):

$$\frac{dE_H}{dS_8^0} = \frac{d}{dS_8^0} \left(E_H^0 + \frac{RT}{4F} \ln \left(f_H \frac{S_8^0}{(S_4^{2-})^2} \right) \right) = \frac{RT}{4F} \frac{1}{S_8^0} \quad (30)$$

$$\frac{dE_H}{dS_4^{2-}} = \frac{d}{dS_4^{2-}} \left(E_H^0 + \frac{RT}{4F} \ln \left(f_H \frac{S_8^0}{(S_4^{2-})^2} \right) \right) = \frac{RT}{4F} \frac{-2}{S_4^{2-}} \quad (31)$$

$$\frac{dE_H}{dS_2^{2-}} = \frac{d}{dS_2^{2-}} \left(E_H^0 + \frac{RT}{4F} \ln \left(f_H \frac{S_8^0}{(S_4^{2-})^2} \right) \right) = 0 \quad (32)$$

$$\frac{dE_H}{dS^{2-}} = \frac{d}{dS^{2-}} \left(E_H^0 + \frac{RT}{4F} \ln \left(f_H \frac{S_8^0}{(S_4^{2-})^2} \right) \right) = 0 \quad (33)$$

On the other hand, the partial derivatives of the overpotential ($\frac{d\eta_H}{dS_i}$) can be derived from linearization with respect to the current intensity (I) and the properties of the battery cell. The linearization equation is presented below:

$$h'_H = \ln \left\{ \frac{I}{2k_1} + \frac{1}{2k_1} \sqrt{I^2 + 4k_1 k'_2} \right\} \quad (34)$$

where

$$\eta'_H = \Omega \bullet \eta_H \quad (35)$$

$$\Omega = \frac{n_e F}{2RT} \quad (36)$$

$$k'_1 = \frac{1}{2} (k_H + k_L m_\phi) \quad (37)$$

$$k'_2 = \frac{1}{2} \left(k_H + \frac{k_L}{m_\phi} \right) \quad (38)$$

$$m_\phi = e^\Phi \quad (39)$$

$$\Phi = \Omega \bullet (E_H - E_L) = \Omega \bullet E_\Delta \quad (40)$$

$$k_H = -2 \bullet i_{H,0} \bullet a_r \quad (41)$$

$$k_L = -2 \bullet i_{L,0} \bullet a_r \quad (42)$$

The parameters in Eqs. (35)–(42) have been previously defined in Table 1. Differentiating Eq. (34) with respect to the sulfur species, we can obtain the following expression for the partial derivatives of the overpotential:

$$\frac{d\eta_H}{dS_i} = \frac{1}{\Omega} \frac{d\eta'_H}{dS_i} \quad (43)$$

$$\frac{d\eta'_H}{dS_i} = \frac{d}{dS_i} \left(\ln \left\{ \frac{I}{2k_1} + \frac{1}{2k_1} \sqrt{I^2 + 4k_1 k'_2} \right\} \right) = \frac{\frac{d}{dS_i} \left(\frac{I}{2k_1} + \frac{1}{2k_1} \sqrt{I^2 + 4k_1 k'_2} \right)}{\frac{I}{2k_1} + \frac{1}{2k_1} \sqrt{I^2 + 4k_1 k'_2}} \quad (44)$$

$$\frac{d\eta'_H}{dS_i} = \frac{\left(\frac{-I}{2k_1^2} - \frac{\sqrt{I^2 + 4k_1 k'_2}}{2k_1^2} + \frac{k'_2}{k_1 \sqrt{I^2 + 4k_1 k'_2}} \right) \frac{dk'_1}{dS_i} + \frac{1}{\sqrt{I^2 + 4k_1 k'_2}} \frac{dk'_2}{dS_i}}{\frac{I}{2k_1} + \frac{1}{2k_1} \sqrt{I^2 + 4k_1 k'_2}} \quad (45)$$

$$\frac{d\eta'_H}{dS_i} = \frac{a \frac{dk'_1}{dS_i} + b \frac{dk'_2}{dS_i}}{c} \quad (46)$$

where the parameters a, b and c are defined as follows:

$$a = \frac{-I}{2k_1^2} - \frac{\sqrt{I^2 + 4k_1 k'_2}}{2k_1^2} + \frac{k'_2}{k_1 \sqrt{I^2 + 4k_1 k'_2}} \quad (47)$$

$$b = \frac{1}{\sqrt{I^2 + 4k_1 k'_2}} \quad (48)$$

$$c = \frac{I}{2k_1} + \frac{1}{2k_1} \sqrt{I^2 + 4k_1 k'_2} \quad (49)$$

Replacing Eq. (46) in the partial derivatives of the voltage, we obtain:

$$\frac{dV}{dS_i} = \frac{d}{dS_i}(E_H + \eta_H) = \frac{dE_H}{dS_i} + \frac{d\eta_H}{dS_i} = \frac{dE_H}{dS_i} + \frac{1}{\Omega} \frac{d\eta'_H}{dS_i} = \frac{dE_H}{dS_i} + \frac{1}{\Omega} \frac{a \frac{dk'_1}{dS_i} + b \frac{dk'_2}{dS_i}}{c} \quad (50)$$

From these expressions, only k'_1 and k'_2 depend on the concentration of sulfur species (S_i), and their partial derivatives are:

$$\frac{dk'_1}{dS_8^0} = \frac{k_L e^{-\Omega E_\Delta} \Omega}{2} \frac{RT}{4F} \frac{1}{S_8^0} \quad (51)$$

$$\frac{dk'_2}{dS_8^0} = \frac{k_L e^{-\Omega E_\Delta} (-\Omega)}{2} \frac{RT}{4F} \frac{1}{S_8^0} \quad (52)$$

$$\frac{dk'_1}{dS_4^{2-}} = \frac{k_L e^{-\Omega E_\Delta} \Omega}{2} \frac{RT}{4F} \frac{-3}{S_4^{2-}} \quad (53)$$

$$\frac{dk'_2}{dS_4^{2-}} = \frac{k_L e^{-\Omega E_\Delta} (-\Omega)}{2} \frac{RT}{4F} \frac{-3}{S_4^{2-}} \quad (54)$$

$$\frac{dk'_1}{dS_2^{2-}} = \frac{k_L e^{-\Omega E_\Delta} \Omega}{2} \frac{RT}{4F} \frac{1}{S_2^{2-}} \quad (55)$$

$$\frac{dk'_2}{dS_2^{2-}} = \frac{k_L e^{-\Omega E_\Delta} (-\Omega)}{2} \frac{RT}{4F} \frac{1}{S_2^{2-}} \quad (56)$$

$$\frac{dk'_1}{dS^{2-}} = \frac{k_L e^{-\Omega E_\Delta} \Omega}{2} \frac{RT}{4F} \frac{2}{S^{2-}} \quad (57)$$

$$\frac{dk_2'}{dS^{2-}} = \frac{k_L}{2} e^{-\alpha E_{\Delta}} (-\Omega) \frac{RT}{4F} \frac{2}{S^{2-}} \quad (58)$$

By replacing the expressions of $\left(\frac{dk_1}{dS_1}\right)$ and $\left(\frac{dk_2}{dS_2}\right)$ in each of the partial derivatives of Eq. (50), the partial derivative of the voltage for each of the sulfur species is obtained.

After obtaining the analytical solutions for the state matrix **A** and the output matrix **C** as explained above, evaluation of observability of the system is possible using Eq. (22). This is analysed by calculating the rank of the matrix as discussed in Section 4.

3.3. Validation of the mathematical model

The mathematical equations for calculating the state matrix **A** and the output matrix **C** have been validated against numerical models. Firstly, a numerical model, developed in MATLAB Simulink, is validated against the predictions from the zero-dimensional model for Li–S batteries [3]. The same model is used to determine numerically the partial derivatives of the voltage. Small disturbances are introduced in the input signal (i.e. mass of the sulfur species), affecting one variable at a time, and the effects on the variation with time of input variables (mass of sulfur species) and output signal (i.e. voltage) are evaluated. This allows to obtain the elements of the **A** and **C** matrices as follows:

$$a_{ij} = \frac{\Delta \left(\frac{dS_i}{dt} \right)}{\Delta S_j} \quad (59)$$

$$c_i = \frac{\Delta V}{\Delta S} \quad (60)$$

where a_{ij} are the terms of the state matrix **A**, c_i are the terms of the output matrix **C**, ΔS is the disturbance introduced in each of the input variables (i.e. mass of sulfur species), $\Delta \left(\frac{dS_i}{dt} \right)$ is the variation in the derivative with time of the input variables, and ΔV is the variation in the voltage generated by ΔS .

4. Results and discussion

4.1. Validation of the numerical model

The numerical model, developed in Simulink, is based on the zero-dimensional model [3] and the linearization of the overpotential with respect to the total current of the system. This model predicts the

evolution of the sulfur species with respect to the time, as well as the voltage. The results from the numerical model are compared to the ones obtained from the zero-dimensional model in a case of discharge at current rate of 0.5C (or 1.7 A). Figs. 2 and 3 present a comparison between the results obtained from both models. According to the results, the voltage and mass of the sulfur species, obtained from the two models, are in a good agreement. When we looked at the zoomed subplots, we can see a bit of difference between the two models, which is related to a small time elapse between them. Actually, there is 8 s elapse between the two models over a simulation of 4000 s of discharge (0.2 % delay). This is caused by the way in which the calculations are performed in the numerical and analytical models. Despite using the same initial conditions for the concentration of the sulfur species (specified in terms of mass percentage), both models predict different values for the mass content of sulfur species at the start of the process ($t = 0$):

Analytical model: $S_0 = [S_8, S_4^{2-}, S_2^{2-}, S^{2-}] = [2.6730, 0.0128, 4.3321 \times 10^{-6}, 1.6321 \times 10^{-6}]$

Numerical model: $S_0 = [S_8, S_4^{2-}, S_2^{2-}, S^{2-}] = [2.6872, 0.0128, 4.4529 \times 10^{-6}, 1.6408 \times 10^{-6}]$

This small difference (0.53 %) in initial mass of the S8 species, leads to the small delay (0.2 %) in the results.

4.2. Validation of the mathematical equations of state matrix **A**

The results obtained from the numerical model, i.e. variation of the sulfur species ($S_i(t)$) and voltage ($V(t)$) in the 0.5C discharge case, are used as a baseline for demonstration of the analytical equations to calculate the state matrix **A** and the output matrix **C**. Numerically calculated values of the state matrix **A** (i.e. Eq. (59)) are compared to the analytical solution, which was presented in Eq. (25). The numerical results calculated for a disturbance value of $\Delta S = 2.7 \times 10^{-10}$, confirm the accuracy of the elements with only three non-zero elements: a_{11} , a_{21} and a_{44} . The values of a_{11} and a_{21} coincide with the value of the shuttle kinetic constant k_s . In addition, a comparison of the analytically and numerically calculated values of element a_{44} is presented in Fig. 4, proving the suitability of the analytical equations for calculation of the state matrix **A**.

4.3. Validation of the mathematical equations of output matrix **C**

For validation of the analytical solution of the output matrix **C**, the numerical solution is developed using Eq. (60). A disturbance ΔS is applied to each of the input variables (i.e. mass of sulfur species, $S_i(t)$)

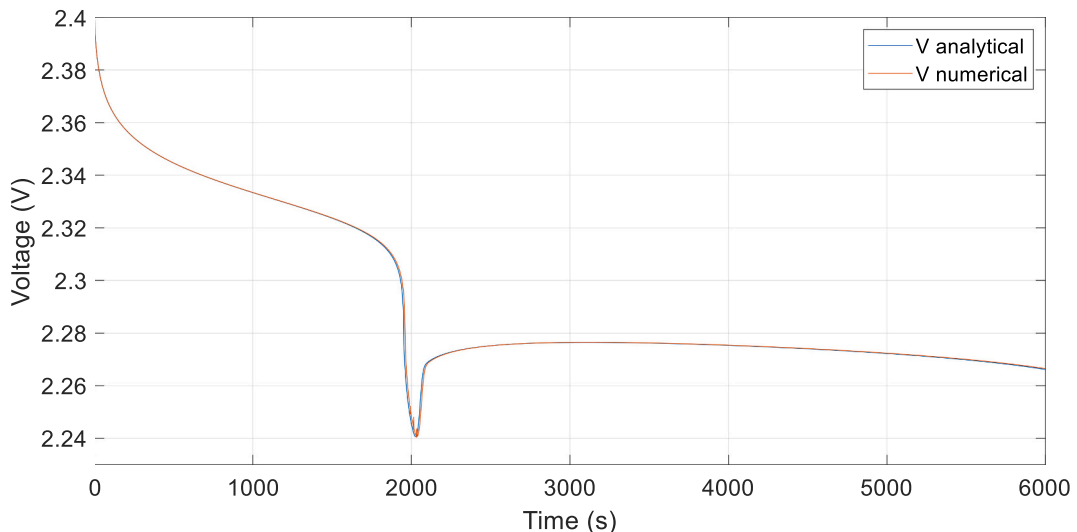


Fig. 2. Comparison of the voltage curve obtained from the zero-dimensional model and the numerical model at discharge rate of 0.5C.

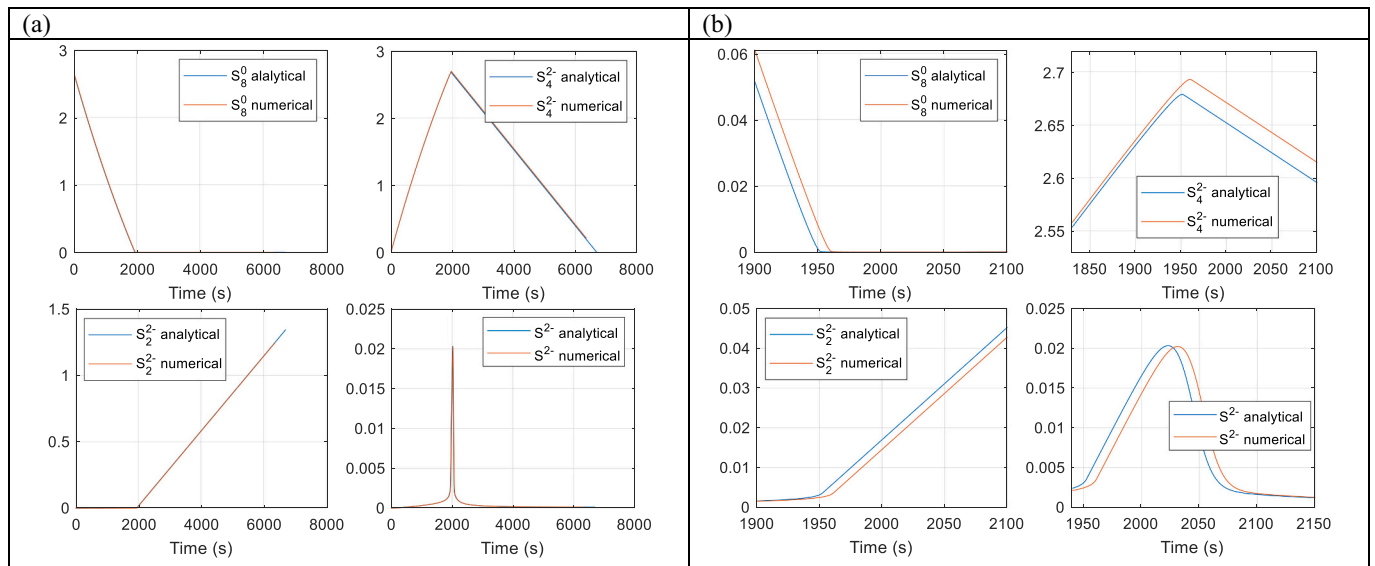


Fig. 3. Comparison of the evolution of the sulfur species with time obtained from the zero-dimensional model and the numerical model at discharge rate of 0.5C: (a) the whole simulation, (b) selected zoomed areas.

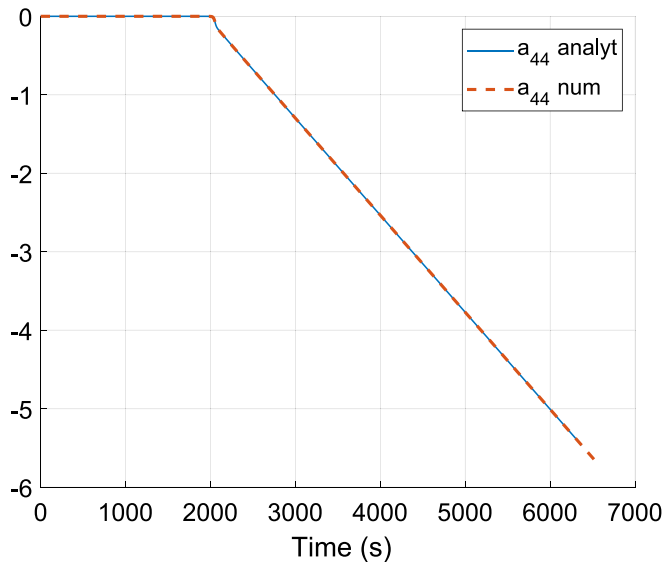


Fig. 4. Comparison between the analytical and numerical solutions of element a_{44} in the state matrix A .

and its effect on the output (i.e. voltage, $V(t)$) is quantified. A sensitivity analysis is conducted on the output of the numerical calculations. The disturbance ΔS is varied, starting from 2.7×10^{-4} and then decreasing in steps of one order of magnitude down to 2.7×10^{-10} when no changes in the results are observed. This sensitivity analysis (shown in Fig. 5) demonstrates that there is a significant difference in the magnitude of three elements of the output matrix C depending on the value of the disturbance. Surprisingly, the element $C_2 \left(\frac{dV}{dS_4^{2-}} \right)$ showed no sensitivity to the disturbance while the element $C_4 \left(\frac{dV}{dS_2^{2-}} \right)$ presents sensitivity in both high and low plateaus.

As with the elements of the state matrix A , variation of the sulfur species with time ($S_i(t)$) obtained from the numerical model in the 0.5C discharge case, were used to corroborate the analytical solution for the elements of the output matrix C . These results are compared to the ones determined using a numerical approach presented in Eq. (60), with a

disturbance value of $\Delta S = 2.7 \times 10^{-10}$ at discharge rate of 0.5C as illustrated in Fig. 6. The results demonstrate a very good correlation between the analytical and the numerical solutions for all the elements. These results are in agreement with the literature such as the work done by Huang et al. [16] in which the zero-dimensional model [3] is studied and the output matrix C is calculated numerically.

4.4. Observability of the Li–S battery model

Analytical calculation of the observability matrix, presented in Eq. (22), and its rank is conducted here by applying the numerical variation of the input variables ($S_i(t)$) and the analytical solutions for A and C . The rank of the observability matrix O resulted in a value of 3 for the discharge process. As it was stated earlier, the system would be observable if the rank of the observability matrix is the same as the order of the state variable. In this study, the state variable ($S_i(t)$) has been defined with order of 4 by considering the four sulfur species. Therefore, we can conclude that the system is not locally observable. This outcome is in accordance to the previous studies based on numerical models or equivalent circuit models that had already identified and reported this problem for Li–S batteries, which leads to shaping a very unique voltage curve for them [15,18]. In the present study, the same result is obtained however, by using a completely different approach.

There are still a few residual irregularities, and it is tempting to explain these away as ‘numerical issues’ – however given the complexity of the mathematics involved, the possibility of small errors should not be disregarded.

5. Conclusions

One of the limitations for commercialisation of the Li–S battery technology is the development of a suitable battery management system for it. That is mainly due to the complexity of Li–S battery's voltage curve, which remains unchanged in a wide range of the battery state of charge (that is within the low-plateau area). As it was demonstrated in this study, such a flat voltage curve makes the system locally unobservable. An analytical evaluation of the observability of a Li–S battery system was presented using a baseline zero-dimensional electrochemical model. For that purpose, analytical equations to determine the state and output matrices were developed and validated against the numerically calculated solutions. The validation results demonstrated a very good

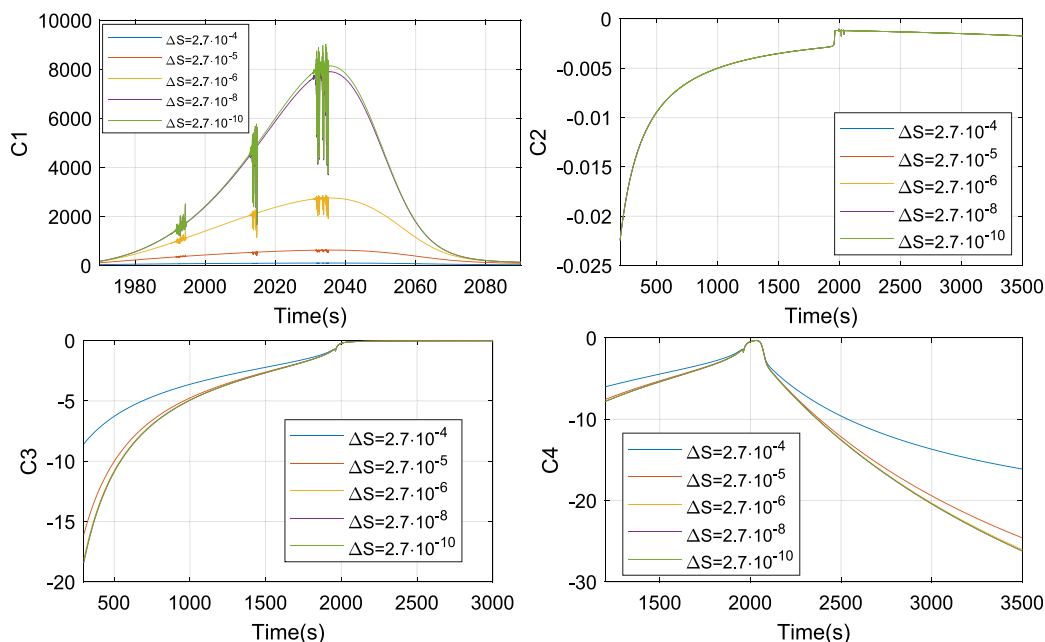


Fig. 5. Sensitivity analysis of the effect of the disturbance on the results of the numerical model in the calculation of the output matrix C.

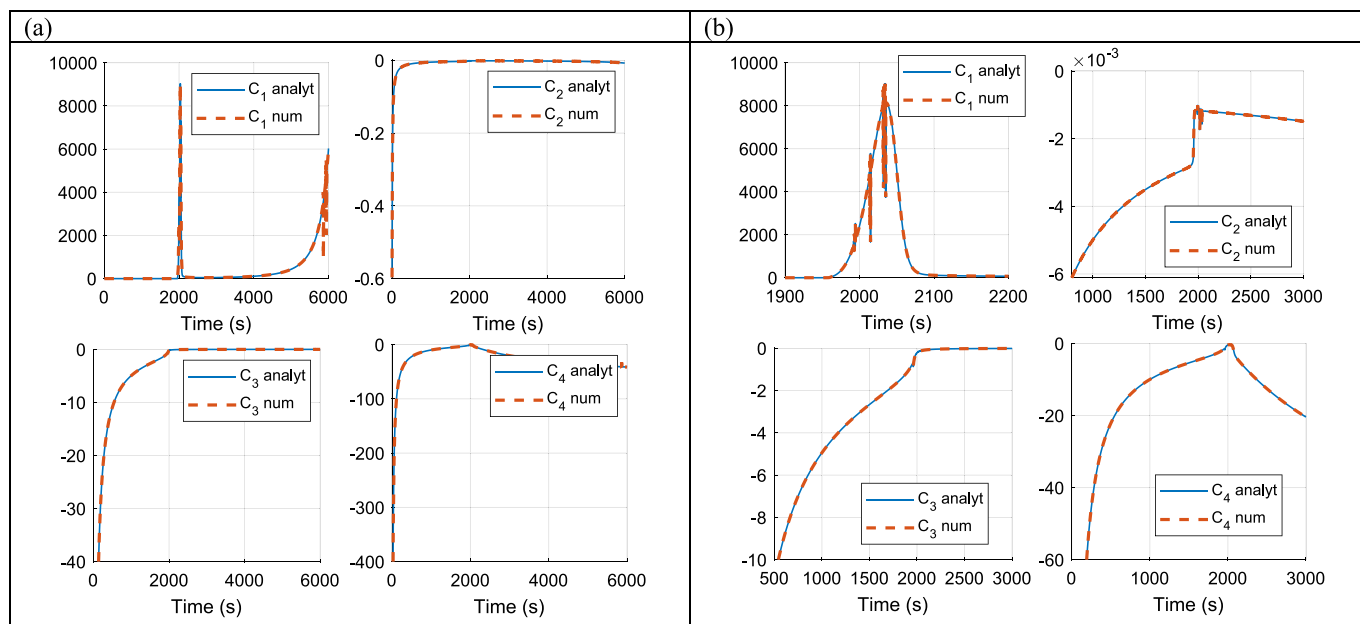


Fig. 6. Comparison of the elements of the output matrix C obtained from the analytical model ('C_i analyt') and the numerical model ('C_i num'): (a) the whole simulation, (b) selected zoomed areas.

match between the two models. In addition, sensitivity of the numerical solution was investigated by applying different levels of disturbance to the input signal. Finally, an observability analysis was performed. According to the observability analysis, the Li-S battery system was shown not to be locally observable, which is in agreement with the previous studies in the literature however, by using a completely different approach.

CRediT authorship contribution statement

Veronica Marchante Rodriguez: Writing – original draft, Validation, Software, Methodology, Formal analysis, Conceptualization. **Neda Shateri:** Writing – original draft, Validation, Software, Methodology,

Formal analysis. **Abbas Fotouhi:** Writing – review & editing, Supervision, Resources. **Karsten Propp:** Software, Methodology, Conceptualization. **Daniel J. Auger:** Writing – review & editing, Supervision, Resources, Funding acquisition.

Declaration of competing interest

The authors declare that they have no known competing financial interests or personal relationships that could have appeared to influence the work reported in this paper.

Data availability

The data that has been used is confidential.

Acknowledgments

The authors thank OXIS Energy for their help and support. This work was funded by the European Commission under grant agreement 814471, and the Innovate UK under grant TS/R013780/1. The data used in this article is described in CORD at [10.17862/cranfield.rd.23904501](https://doi.org/10.17862/cranfield.rd.23904501).

References

- [1] M. Yan, W.-P. Wang, Y.-X. Yin, L.-J. Wan, Y.-G. Guo, Interfacial design for lithium–sulfur batteries: from liquid to solid, *EnergyChem* 1 (1) (Jul. 2019) 100002, <https://doi.org/10.1016/j.enchem.2019.100002>.
- [2] A. Fotouhi, D.J. Auger, L. O'Neill, T. Cleaver, S. Walus, Lithium-sulfur battery technology readiness and applications—a review, *Energies* 10 (12) (Dec. 2017) 12, <https://doi.org/10.3390/en10121937>.
- [3] M. Marinescu, T. Zhang, G.J. Offer, A zero dimensional model of lithium–sulfur batteries during charge and discharge, *Phys. Chem. Chem. Phys.* 18 (1) (Dec. 2015) 584–593, <https://doi.org/10.1039/C5CP05755H>.
- [4] T. Cleaver, P. Kovacic, M. Marinescu, T. Zhang, G. Offer, Perspective—commercializing lithium sulfur batteries: are we doing the right research? *J. Electrochem. Soc.* 165 (1) (2018) A6029–A6033, <https://doi.org/10.1149/2.0071801jes>.
- [5] S. Dörfler, et al., Recent progress and emerging application areas for lithium–sulfur battery technology, *Energy Technol. Weinh. Ger.* 9 (1) (Jan. 2021) 2000694, <https://doi.org/10.1002/ente.202000694>.
- [6] Y.V. Mikhaylik, J.R. Akridge, Polysulfide shuttle study in the Li/S battery system, *J. Electrochem. Soc.* 151 (11) (Oct. 2004) A1969, <https://doi.org/10.1149/1.1806394>.
- [7] K. Kumaresan, Y. Mikhaylik, R.E. White, A mathematical model for a lithium–sulfur cell, *J. Electrochem. Soc.* 155 (8) (Jun. 2008) A576, <https://doi.org/10.1149/1.2937304>.
- [8] M. Zhang, L. Marinescu, M. Wild O'Neill, G. Offer, Modeling the voltage loss mechanisms in lithium–sulfur cells: the importance of electrolyte resistance and precipitation kinetics, *Phys. Chem. Chem. Phys.* 17 (35) (Aug. 2015) 22581–22586, <https://doi.org/10.1039/C5CP03566J>.
- [9] M. Ghaznavi, P. Chen, Analysis of a mathematical model of lithium-sulfur cells part III: electrochemical reaction kinetics, transport properties and charging, *Electrochim. Acta* 137 (Aug. 2014) 575–585, <https://doi.org/10.1016/j.electacta.2014.06.033>.
- [10] T. Zhang, M. Marinescu, S. Walus, G.J. Offer, Modelling transport-limited discharge capacity of lithium-sulfur cells, *Electrochim. Acta* 219 (Nov. 2016) 502–508, <https://doi.org/10.1016/j.electacta.2016.10.032>.
- [11] K. Yoo, M.-K. Song, E.J. Cairns, P. Dutta, Numerical and experimental investigation of performance characteristics of lithium/sulfur cells, *Electrochim. Acta* 213 (Sep. 2016) 174–185, <https://doi.org/10.1016/j.electacta.2016.07.110>.
- [12] Y.X. Ren, T.S. Zhao, M. Liu, P. Tan, Y.K. Zeng, Modeling of lithium-sulfur batteries incorporating the effect of Li₂S precipitation, *J. Power Sources* 336 (Dec. 2016) 115–125, <https://doi.org/10.1016/j.jpowsour.2016.10.063>.
- [13] A.F. Hofmann, D.N. Fronczek, W.G. Bessler, Mechanistic modeling of polysulfide shuttle and capacity loss in lithium–sulfur batteries, *J. Power Sources* 259 (Aug. 2014) 300–310, <https://doi.org/10.1016/j.jpowsour.2014.02.082>.
- [14] C. Xiong, T.S. Zhao, Y.X. Ren, H.R. Jiang, X.L. Zhou, Mathematical modeling of the charging process of Li-S batteries by incorporating the size-dependent Li₂S dissolution, *Electrochim. Acta* 296 (Feb. 2019) 954–963, <https://doi.org/10.1016/j.electacta.2018.11.159>.
- [15] . Fotouhi, D. J. Auger, K. Propp, and S. Longo, 'Lithium–sulfur battery state-of-charge observability analysis and estimation', *IEEE Trans. Power Electron.*, vol. 33, no. 7, pp. 5847–5859, Jul. 2018, doi:<https://doi.org/10.1109/TPEL.2017.2740223>.
- [16] Z. Huang, D. Zhang, L.D. Couto, Q.-H. Yang, S.J. Moura, State Estimation for a Zero-Dimensional Electrochemical Model of Lithium-Sulfur Batteries, *ArXiv210110436 Cs Eess*, Jan. 2021. Accessed: Apr. 28, 2021. [Online]. Available: <http://arxiv.org/abs/2101.10436>.
- [17] C. Xu, et al., Online state estimation for a physics-based Lithium-Sulfur battery model, *J. Power Sources* 489 (Mar. 2021) 229495, <https://doi.org/10.1016/j.jpowsour.2021.229495>.
- [18] . Fotouhi, D. J. Auger, K. Propp, S. Longo, Electric vehicle battery parameter identification and SOC observability analysis: NiMH and Li-S case studies, *IET Power Electron.* 10 (11) (2017) 1289–1297, <https://doi.org/10.1049/iet-pel.2016.0777>.
- [19] *Numerical Methods in General*, in: E. Kreyszig (Ed.), *Advanced Engineering Mathematics*, Wiley, New York, 1993.
- [20] C. Hu, et al., In situ wrapping of the cathode material in lithium-sulfur batteries, *Nat. Commun.* 8 (1) (Sep. 2017) 1, <https://doi.org/10.1038/s41467-017-00656-8>.
- [21] Z. Zeng and X. Liu, 'Sulfur immobilization by "chemical anchor" to suppress the diffusion of polysulfides in lithium–sulfur batteries', *Adv. Mater. Interfaces*, vol. 5, no. 4, p. 1701274, 2018, doi:<https://doi.org/10.1002/admi.201701274>.
- [22] J.B. Robinson, et al., 2021 roadmap on lithium sulfur batteries, *J. Phys. Energy* 3 (2021) 031501.
- [23] *Toward Rigorous Validation, of Li-S Battery Models*, M. Cornish, M. Marinescu, *J. Electrochem. Soc.* 169 (6) (2022).

2024-03-29

Deterministic observability calculations for zero-dimensional models of lithium sulfur batteries

Rodriguez, Veronica M.

Elsevier

Rodriguez VM, Shateri N, Fotouhi A, et al., (2024) Deterministic observability calculations for zero-dimensional models of lithium sulfur batteries. *Journal of Energy Storage* 2024, Article Number 111442

<https://doi.org/10.1016/j.est.2024.111442>

Downloaded from Cranfield Library Services E-Repository